JOURNAL OF MATERIALS SCIENCE **38** (2003) 2987–2991

Heat treatment temperature effects on structural and electrochemical properties of PVDC-based disordered carbons

CHAN KIM, KAP SEUNG YANG*
Faculty of Applied Chemical Engineering, Chonnam National University,
300 youngbong-dong, Buk-gu, Gwangju 500-757, South Korea
E-mail: ksyang@chonnam.ac.kr

Y. J. KIM, M. ENDO
Faculty of Engineering, Shinshu University, 500 Wakasato, Nagano 380-0922, Japan

X-ray diffraction (XRD), BET surface area, Raman spectroscopy and electrochemical measurement were used to investigate the morphological behaviors of poly(vinylidene chloride) (PVDC)-based carbons in the heat treatment temperature range 700 to 3000°C. X-ray diffraction and Raman scattering results proposed that PVDC-based carbons heat treated up to 3000°C behaved as typically non-graphitizable carbons. The structural parameters were correlated with discharge/charge characteristics of Li ions into PVDC-based carbons. It was realized that the Li ion storage capacity of PVDC-based carbons during the first cycle tended to decrease with increasing the heat-treatment temperature due to the reduction of hydrogen content and the reduction of the specific surface area from pores. © *2003 Kluwer Academic Publishers*

1. Introduction

Nowadays Li-ion secondary batteries are recognized as the standard energy storage device for portable electronics, and these batteries are superior when compared with other conventional batteries such as Lead acid, NiCd and NiMH, because of their high power and high energy density [1]. They were first developed and commercialized by Sony in 1991 and have been used for a wide range of portable devices, such as notebook computers, cellular phones and digital video cameras, etc. These developments in technology and the commercialization of the Li-ion secondary batteries result from the use of well-designed carbon and graphite materials as anodes. Various types of carbon and graphite materials have been extensively examined as possible anode materials in Li-ion secondary batteries. Some of them are now used for the construction of Li-ion secondary batteries. Typically, highly-ordered graphite, heat-treated at temperatures as high as 3000°C, and non-graphitizable carbon, heat treated at temperatures as low as 1200°C, have been used in anodes for commercial batteries. At present, non-graphitizable carbon has attracted more attention as an anode material because of its low cost and higher capacity when compared with graphite anodes [1–5]. Therefore, the elucidation of the lithium insertion mechanism and the improvement of the irreversible capacity of non-graphitizable carbons are important issues.

Porous carbon materials have attracted interest as high-performance materials for electrode applications because of the special pore structure that is responsible for their electric double layers and their relatively high conductivity. Recently, much attention has been focused on electrodes for electrical double layer capacitors (EDLC) based on organic polymer materials. It has been found that poly(vinylidene chloride) (PVDC), heat treated at only at about 700°C exhibits a capacitance of 100F/g [6].

However, the structural characterization and electrochemical properties of PVDC-based carbons, heat treated at temperatures up to 3000°C, have not yet been reported. In this work, we report the correlations between the structural parameters and the electrochemical properties of PVDC-based carbons heat treated at various temperatures. The microstructural characteristics of PVDC-based carbons prepared at various temperatures were examined on the basis of X-ray diffraction (XRD), BET surface area analysis, and Raman spectroscopy.

2. Experimental

Temperature-programmed heating of PVDC polymer sample (100 mg) was performed in a Thermal Sciences STA 1500 thermogravimetric analyzer (TG-MS) at a heating rate of 1°C/min. The gases evolved were sampled by using a heated silica capillary which connected

---

*Author to whom all correspondence should be addressed.

the TGA instrument to the mass spectrometer and analyzed by using a VG Quadrupoles 300 amu mass spectrometer.

PVDC-based carbon samples were prepared by heat-treatment at various temperatures 700 to 3000°C under a flow of high purity argon gas (99.999%). A conventional resistance furnace was used for heat-treatment below 1000°C, and a graphite resistance furnace was used for heat treatment above 1000°C for 1 h at each terminal temperature.

Thermal stability of the samples was measured by thermogravimetric analysis (TGA) (STA 1640, Stanton Redcroft). X-ray diffractometer (Rigaku Geigerflex, 30 kV, 40 mA) with a Cu K_α ($\lambda = 0.15406$ nm) X-ray source was used to measure the Bragg diffraction from each carbon sample. The d_{002} value was calculated on the basis of the Bragg Equation with the diffraction angle determined by drawing a line parallel, tangential to the peak to the base line and the full width at half maximum (FWHM) for $L_{c(002)}$ was also determined with reference to a line constructed parallel to the base line.

Raman spectra were taken at room temperature under ambient conditions using a Renishaw Image Microscope System 1000 equipped with a charge-coupled device (CCD) multichannel detector. The excitation source was a 514.5 nm Ar-ion laser line and the optical power at the sample position was maintained at 10 mW. The scattered light was collected in a backscattering configuration. The first-order (1000–1800 cm^{-1}) Raman spectra were recorded at a 2.0 cm^{-1} resolution. The spectra were averaged over three scans to improve the signal-to-noise ratio, and the data were corrected for the spectral response of the instrument.

Multipoint Brunauer-Emmett-Teller (BET) surface area measurements were made with a Gemini II surface area analyzer, based on a flowing gas technique. About 150 mg of sample was weighed, placed in a Pyrex sample holder and degassed at 250°C for 2 h prior to the measurements previously used nitrogen gas.

Electrochemical performances were performed with three-electrode test cells made of pyrex glass. The working electrodes were prepared by dispersing the carbon samples (95 wt%) with poly(vinylidene fluoride) (PVDF) (5 wt%), using 1-methyl-2pyrrolidinone as a solvent. Approximately 1 mg of paste-like mixture was spread thinly onto a nickel mesh (5 mm × 5 mm) and pressed at a pressure of 2 MPa. The electrode was then vacuum dried for 48 h at 90°C. After drying, the electrode was transferred to an Ar glove box, without exposing the electrode to air. Lithium metal was used both as a counter electrode and as a reference electrode. The electrolyte employed was a *1M* solution of $LiClO_4$ dissolved in a 50/50 volumetric mixture of ethylene carbonate (EC) and diethyl carbonate (DEC). The specific capacity of the carbon electrode was measured by a potentiostat/galvanostat (Hokuto Denko Co., Ltd., HA-151) during the charge and discharge cycles in the ranges 0 to 2.8 V, at a current density of 30 mA/g-carbon. All the operations of the cell assembly were carried out in a glove box filled with high purity argon gas containing lower than 1 ppm of water or oxygen.

3. Results and discussion

Fig. 1 shows the results of the thermogravimetric (TGA) analysis for poly-vinylidene chloride (PVDC, $-(CH_2CCl_2)_n-$) under nitrogen gas flow. Dramatic weight losses of the sample occurred twice at about 250°C and 500°C (indicated by arrows in Fig. 1), resulting in a carbon yield of 24% at 800°C. The weight loss at about 250°C was mainly revealed by the evolution of Cl, HCl indicated by 35 and 36 amu respectively, and the weight loss at about 500°C was related to evolution of hydocarbons from the PVDC (Fig. 2).

Fig. 3 shows the BET surface area of PVDC-based carbons as a function of heat-treatment temperature (HTT) from 700°C to 3000°C. For HTT $\leqq$ 1000°C, the BET surface area decreases relatively slowly with an increase in temperature. Between 1000°C and 2000°C, the BET surface area decreases dramatically. For HTT $\geqq$ 2000°C, the BET surface area remains essentially constant at about 3 m^2/g.

Fig. 4 shows the XRD patterns of PVDC-based carbons at various heat-treatment temperatures experimented. There are two broad diffraction peaks around 2θ of 24° and 44° in each spectrum, corresponding to the diffraction of (002) plane and (100)/(101) of graphite structure, respectively [7, 8]. The peak

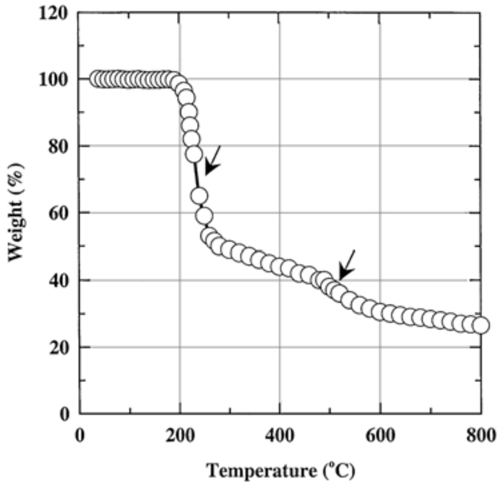

Figure 1 The results of themogravimetric analysis for PVDC flow of N_2 gas.

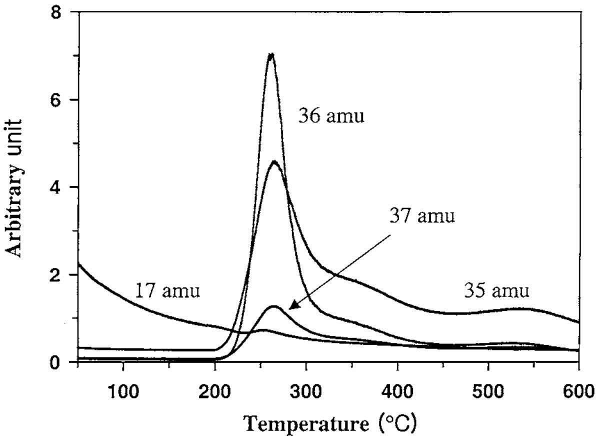

Figure 2 The concentrations of evolved gases from PVDC as a function of temperature.

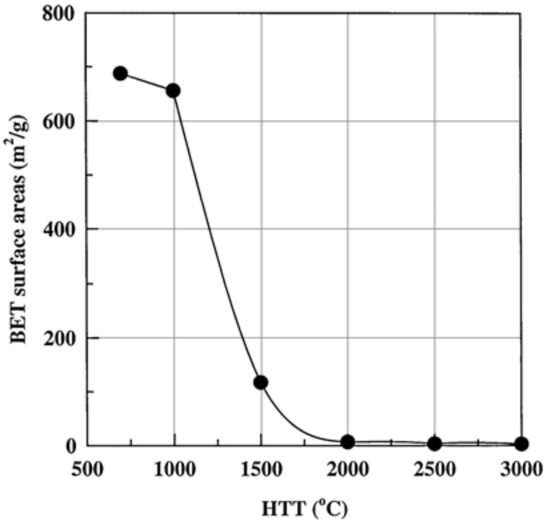

Figure 3 BET surface area of PVDC-based carbons as a function of HTT from 700°C to 3000°C.

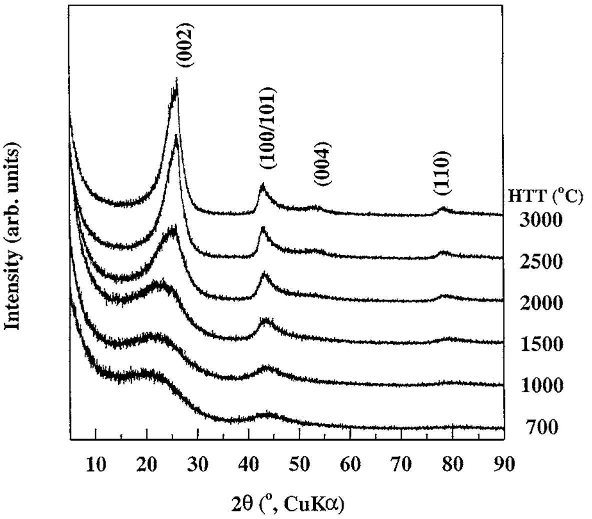

Figure 4 XRD patterns of PVDC-based carbons as a function of heat-treatment temperature (HTT) from 700°C to 3000°C.

representing (002) plane slightly sharpens and upshifts with increasing HTT, and the absence of the (112) peak at 2θ of 83° even at 3000°C indicates the presence of a non-graphitizable carbonaceous structure [9].

Fig. 5 shows the HTT dependences of the interlayer spacing d_{002} and Fig. 6 shows variations of crystallite size in the directions of stacking height $L_{c(002)}$ and plane $L_{a(100)}$, as determined by the XRD measurements. The crystallite parameters L_c and L_a were calculated on the basis of Scherrer's equations [10, 11]

$$L_c = \frac{(0.91)\lambda}{\beta\cos\theta}, \quad L_a = \frac{(1.84)\lambda}{\beta\cos\theta}$$

where β is the full width at half-maximum intensity of the diffraction peak in radian, θ is the Bragg angle, and λ is the X-ray wavelength.

The d_{002} value decreases considerably with increasing HTT, approaching to the value of graphite, as shown in Fig. 5. It needs to be noted that the three structural parameters, d_{002}, $L_{c(002)}$ and $L_{a(100)}$, show essentially no changes above 2500°C HTT (Fig. 6), differently from graphitizable carbons. The $L_{c(002)}/L_{a(100)}$ values of 1.2 nm/4.6 nm increased a factor of almost 4 to become 4.5 nm/16.5 nm, respectively, when the HTT increased from 700°C to 3000°C.

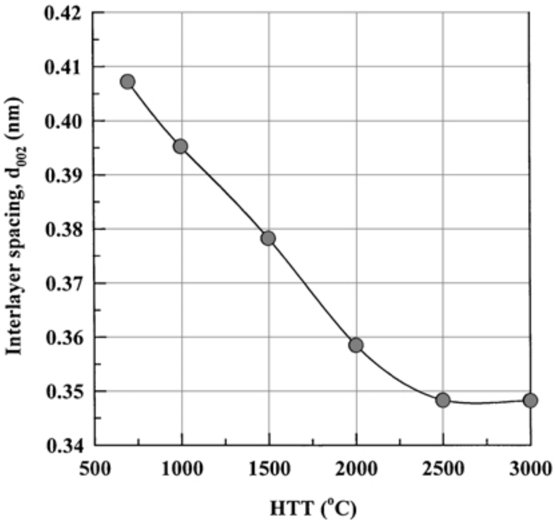

Figure 5 Interlayer spacing, d_{002} of PVDC-based carbons as a function of HTT from 700°C to 3000°C.

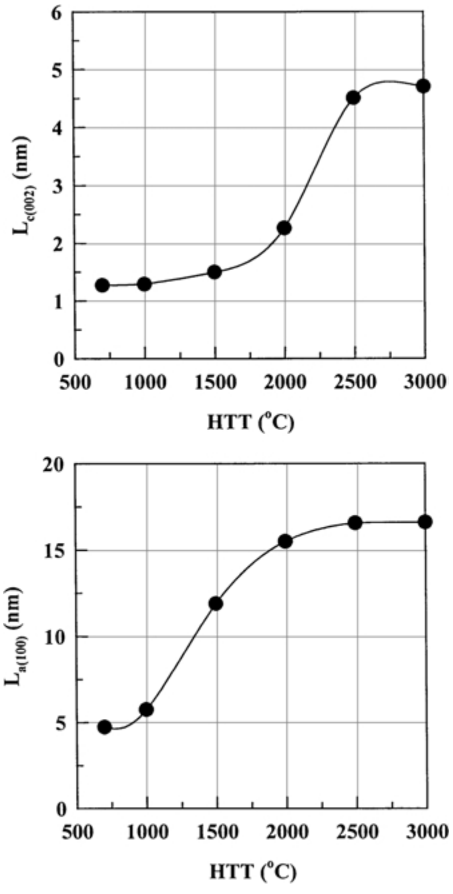

Figure 6 Crystallite thickness, $L_{c(002)}$ and width $L_{a(100)}$ of PVDC-based carbons as a function of HTT from 700°C to 3000°C.

Fig. 7 demonstrates the first-order Raman spectra of PVDC-based carbons as a function of HTT. With increasing HTT, the samples show an increase in the Raman intensity and a decrease in the line-width of the graphitic 1580 cm^{-1} peak (G-band). Above 2500°C, PVDC-based carbons show a dramatic

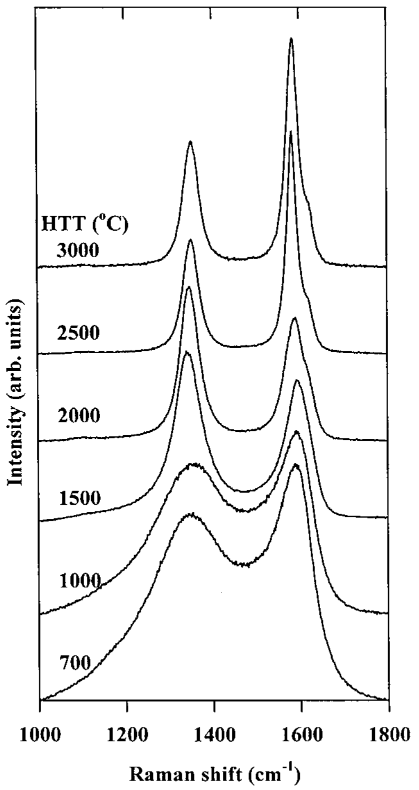

Figure 7 The first-order Raman spectra of PVDC-based carbons as a function of HTT from 700°C to 3000°C.

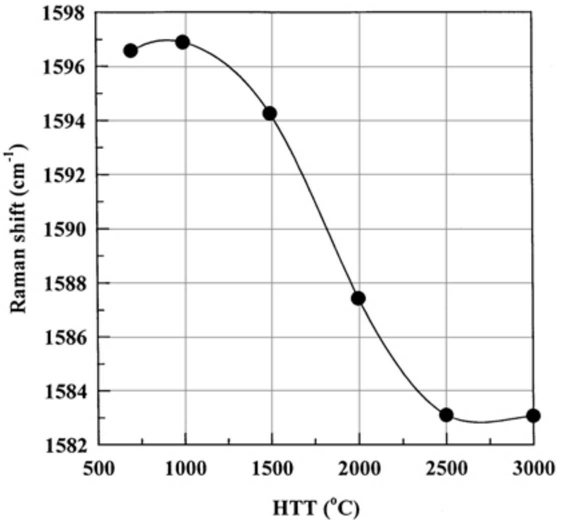

Figure 8 Plot of the G-band position of PVDC-based carbons as a function of HTT from 700°C to 3000°C.

decreases in both the integrated Raman intensity and line-width of the disorder-induced 1355 cm^{-1} peak (D-band), as compared with those of the 1580 cm^{-1} peak (G-band). Above 2000°C, a well-defined 1620 cm^{-1} peak (D-band) appears to indicate formation of condensed aromatic planes and an increase in the crystallite size during the heat-treatment.

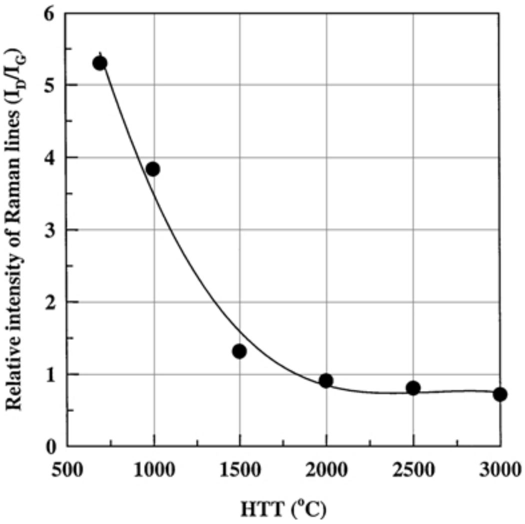

Figure 9 Plot of the relative intensity, $R = I_D/I_G$, of PVDC-based carbons as a function of HTT from 700°C to 3000°C.

Fig. 8 shows the shift of the Raman G-band of PVDC-based carbons as a function of HTT. No significant shift was observed at HTT $\leqq$ 1000°C, and then the band shifts dramatically downfield above 1000°C. At HTT $\geqq$ 2500°C, the G-band position approaches to 1583 cm^{-1}. These phenomena are associated with the development of graphite microcrystallites in the denatured PVDC for HTT $\geqq$ 2500°C, where the d_{002} spacing exhibits values larger than 0.344 nm indicating the presence of a turbostratic carbonaceous structure.

HTT effect on relative intensity, R (I_D/I_G), is shown in Fig. 9. The value of R decreases with an increasing HTT suggesting that structural changes are occurring in PVDC-based carbon as HTT increases. For HTT $\leqq$ 1500°C, the R value decreases sharply, while the Raman shift of the G-band is steady, as shown in Fig. 8. These results would come from the simultaneous changes in chemistry and morphology of the carbon resulting from loss of HCl, H_2, CH_4 etc., in this temperature range. The decrease in the R-value would be closely related to improve in ordering of condensed aromatic layers.

Fig. 10 demonstrates the typical discharge/charge curves for PVDC-based carbons at various HTTs, and the numerical data are summarized in Table I. Within the present series of samples, the sample at HTT of 700°C shows the largest hysteresis in its voltage profile. These phenomena are related the Li remaining after the chemical reactions of Li with hydrogen atoms and depositions as Li metal clusters rather than as Li ions in the relatively large pores of PVDC based carbon [4]. The first charge capacities of PVDC-based carbons are very low in comparison with that of the theoretical capacity (Li-graphite intercalation compounds, 372 mAh/g). The irreversible capacities decrease with increasing HTT, as shown in Table I. The result would

TABLE I Discharge/charge capacities of PVDC-based carbons at various heat-treatment temperatures

	Discharge capacity (mAh/g)		Charge capacity (mAh/g)		Irreversible capacity loss (mAh/g)	
HTT (°C)	1st	2nd	1st	2nd	1st	2nd
700	596	225	200	188	396	36
1000	491	167	144	143	346	24
1500	205	114	108	103	97	11
2000	178	117	106	105	72	11
2500	178	121	113	110	65	11
3000	178	125	114	114	64	11

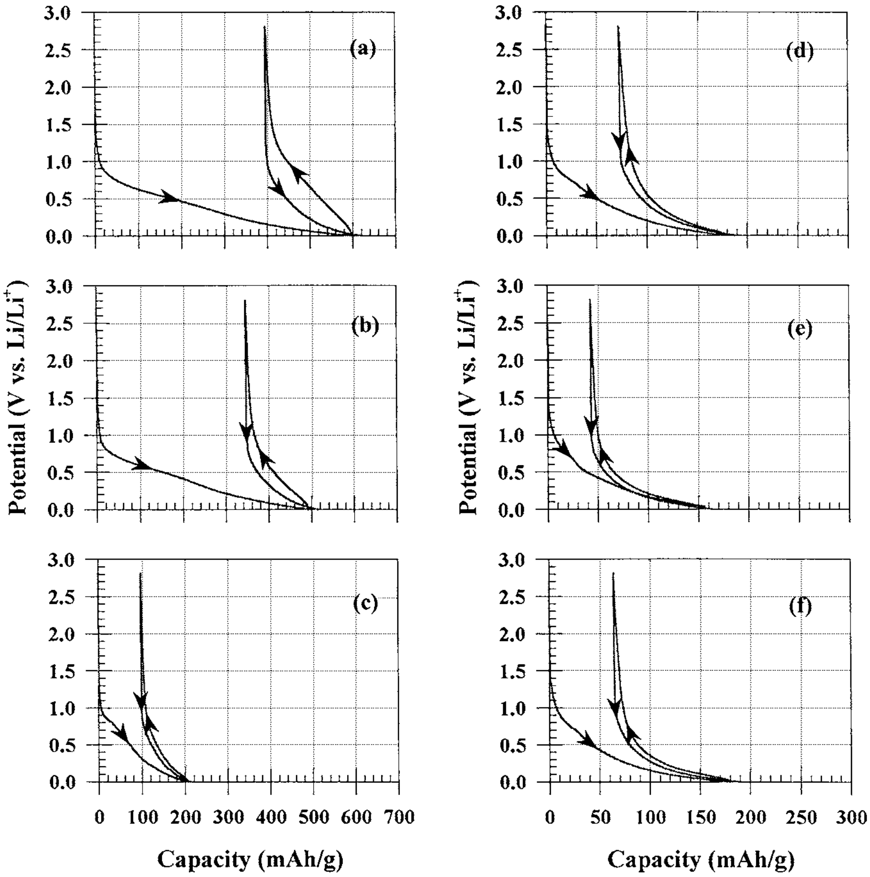

Figure 10 Discharge/charge curves of PVDC-based disordered carbons as a function of HTT: (a) HTT = 700°C, (b) HTT = 1000°C, (c) HTT = 1500°C, (d) HTT = 2000°C, (e) HTT = 2500°C, and (f) HTT = 3000°C.

come from the reduction of Li metal deposition due to the reduced porosity in the PVDC based carbons above 1000°C [13–15].

4. Conclusions

This study presents the X-ray diffraction, BET surface area, Raman spectroscopy, and electrochemical measurements to characterize PVDC-based carbonaceous materials obtained at various heat-treatment temperatures. The PVDC-based carbons heat treated up to 3000°C typically represent non-graphitizable carbon features, showing decrease in hysteresis of charge/discharge capacity with increasing heat-treatment temperature. The irreversible capacity between the first discharge and charge following cycles was correlated with the Raman R-values in these materials. The PVDC carbon would be desirable for EDLC electrode on the basis of the structural behaviors by heat treatments at optimum temperature in aiming maximum specific capacitance through matching specific surface area and electrical conductivity.

References

1. M. ENDO, C. KIM, K. NISHIMURA, T. FUJINO and K. MIYASHITA, *Carbon* **38** (2000) 183.
2. M. ENDO, C. KIM, T. KARAKI, T. FUJINO, M. J. MATTHEWS, S. D. M. BROWN and M. S. DRESSELHAUS, *Synthetic Metals* **98** (1998) 17.
3. T. ZHENG, Y. LIU, E. W. FULLER, S. TSENG, U. VON. SACKEN and J. R. DAHN, *J. Electrochem. Soc.* **142** (1995) 2581.
4. E. DUIEL, A. E. GEORGE and J. R. DAHN, *ibid.* **145** (1998) 2252.
5. T. ZHENG, Q. ZHONG and J. R. DAHN, *ibid.* **142** (1995) L211.
6. T. TAKEDA and M. ENDO, *Tanso* **189** (1999) 179 (in Japanese).
7. V. S. BABU and M. S. SEEHRA, *Carbon* **34** (1996) 1259.
8. M. S. SEEHRA and A. S. PAVLOVIC, *ibid.* **31** (1993) 557.
9. M. ENDO, C. KIM, T. HIRAOKA, T. KARAKI, N. NISHIMURA, M. J. MATTHEWS, S. D. M. BROWN and M. S. DRESSELHAUS, *J. Mater. Res.* **13** (1998) 2023.
10. W. RULAND, in "Chemistry and Physics of Carbon," edited by P. L. Walker, Jr. (Marcel Deeker, New York) Vol. 7, p. 1.
11. R. PERRET and W. RULAND, *J. Appl. Cryst.* **1** (1968) 257.
12. H. P. KLUG and L. E. ALEXANDER, "X-ray Diffraction Procedures" (John Wiley & Sons, New York, 1974) p. 667, and references therein.
13. A. SATOH, N. TAKAMI and T. OHSAKI, *Solid State Ionics* **80** (1995) 291.
14. M. WAKIHARA, *Functi. Mater.* **14** (1994) 5.
15. R. KOSTECKI, T. TRAN, X. SONG, K. KINOSHITA and F. MCLARNON, *J. Electrochem. Soc.* **144** (1997) 3111.

Received 24 July 2001
and accepted 10 April 2003